Lu Y, Wang Y, Bao H, Yuan Y, Wang L, Roskilly AP.

Analysis of an optimal resorption cogeneration using mass and heat recovery processes.

***Applied Energy* 2015, 160, 892–901.**

Analysis of an optimal resorption cogeneration using mass and heat recovery processes

Yiji Lu [a,*], Yaodong Wang [a], Huashan Bao [a],

Ye Yuan [a], Liwei Wang [b], Anthony Paul Roskilly [a]

[a] Sir Joseph Swan Centre for Energy Research, Newcastle University, Newcastle, NE1 7RU, UK.

[b] Institute of Refrigeration and Cryogenics, Shanghai Jiao Tong University, Shanghai, 200240, China;

Highlights

Resorption cogeneration for electricity and refrigeration generation

Mass and heat recovery to further improve the performance

The first and second law analysis

Abstract

This paper presents an optimised resorption cogeneration using mass and heat recovery to improve the performance of a novel resorption cogeneration fist proposed by Wang et al. This system combines ammonia-resorption technology and expansion machine into one loop, which is able to generate refrigeration and electricity from low-grade heat sources such as solar energy and industrial waste heat, etc. Two sets of resorption cycle are designed to overcome the intermittent performance of the chemisorption and produce continuous/simultaneous refrigeration and electricity. In this paper, twelve resorption working pairs of salt complex candidates are analysed by the first law analysis using Engineering Equation Solver (EES). The optimal resorption working pairs from the twelve

* Corresponding author. Tel.:+44 (0)191-246-4849
E-mail address: y.j.lu@ncl.ac.uk

candidates under the driven temperature from 100 °C to 300 °C are identified. By applying heat/mass recovery, the coefficient of performance (COP) improvement is increased by 38% when the high temperature salt (HTS) is $NiCl_2$ and by 35% when the HTS is $MnCl_2$. On the other hand, the energy efficiency of electricity has also been improved from 8% to 12% with the help of heat/mass recovery. The second law analysis has also been applied to investigate the exergy utilisaion and identify the key components/processes. The highest second law efficiency is achieved as high as 41% by the resorption working pair $BaCl_2$-$MnCl_2$ under the heat source temperature at 110 °C.

Keywords: resorption cogeneration, refrigeration and electricity, resorption working pair, heat and mass recovery, first law analysis, second law analysis

---

Nomenclature

COP	Coefficient of performance
Cp	Specific heat at constant pressure (KJ/kg·K)
E	Exergy (kJ/kg)
HTS	High temperature salt
h	Specific enthalpy (kJ/kg)
LTS	Low temperature salt
m	Mass flow rate (kg/s)
P	Pressure (kPa)
Q	Heat (kW)
T	Temperature (K)
u	Specific internal energy (kJ/kg)
W	Power output from expander (kW)
Greek letters	
ρ	density (kg/m3)
η	efficiency
Δx	adsorption/desorption quantity (kg/kg)
Subscripts	
am	ammonia
ele	electricity
hr	heat recovery
mr	mass recovery
ref	refrigeration
tot	total

1. Introduction

To reduce the energy consumption of conventional energies, using low-grade heat such as solar energy, industrial waste heat, and geothermal energy attracts ever increasing attentions. The most widely applied energy conversion system is the Rankine cycle, which can generate extra work from low-grade heat source. The efficiency of the Rankine cycle highly depends on the heat source temperature and heat sink temperature. However, the isothermal endothermic and exothermic processes cannot perfectly match the variable temperature of the heat source and heat sink. The Kalina cycle is then proposed by Kalina using ammonia-water as working fluid in 1983 [1], which allows adjustable supply temperature by controlling the concentration of the ammonia-water [2-5]. Compared with the conventional Rankine cycle, the Kalina cycle can give up to 32% more power and produce 10% to 20% higher exergy efficiency when the heat source temperature is lower than 537 ^{o}C[6]. To further improve the exergy efficiency, Goswami developed the Kalina cycle into a combined power and refrigeration system by adding a heat exchanger at the outlet of the expansion machine to retrieve refrigeration[7-9]. However, this cogeneration system suffers from its low refrigeration production, which can only achieve the refrigeration coefficient of performance (COP) at 0.0125[9].

Resorption is an advanced adsorption technology first proposed and adopted by thermochemical system since 1993 [10]. Resorption system mainly contains two adsorbent beds filled with two different salts. Under the same working pressure, the salt which reacts at lower temperature is called as low temperature salt (LTS), and the other is named as high temperature salt (HTS). Resorption technology uses the desorption heat of the salt to yield refrigeration while the conventional adsorption uses the latent heat of ammonia. Because the desorption heat of salt is almost twice of the latent heat of ammonia, the theoretical cooling capacity of resorption system is larger than that of conventional adsorption system [11, 12]. The varied selection of chloride salts which can reversibly

react with ammonia allows the resorption cogeneration powered by various temperature sources[13]. Furthermore, no condenser and evaporator are required in resorption system, which enlarges the application of the system under vibration conditions such as heavy duty vehicle, fish boat, etc[14].

Liwei Wang et al. first proposed a resorption cogeneration producing power and refrigeration[15]. This originally proposed system shows attractive performance compared with the Goswami cycle under the super heater temperature from 150 ^{o}C to 400 ^{o}C at 10 ^{o}C refrigeration temperature. In this work, an optimal resorption cogeneration system is proposed to further improve the performance by using heat and mass recovery processes. Heat and mass recovery processes have been theoretically analysed and experimentally investigated by many researchers from the 1980s in several chemisorption systems [16-20], which showed considerable improvement with the application of those two methods. In order to have an overall understanding of the resorption cogeneration, the first law analysis is applied to choose the optimal resorption working pair from the twelve candidates under the temperature ranging from 100 ^{o}C to 300 ^{o}C. To investigate the effect of the heat recovery process, mass recovery process and combined heat/mass recovery processes, four optimal resorption working pairs are further analysed by the first and second law analysis.

2. An optimal resorption cogeneration system

2.1 Principle of the resorption cogeneration

The resorption cogeneration includes two high temperature salts (HTS), two low temperature salts (LTS), an expander, a separated circulator for heat recovery and some accessories. This system is able to provide continuous electricity and refrigeration by switching it between step 1 to step 2, which is shown in Fig.1.

In step 1, V_1, V_3, V_5, V_{m1}, V_{m2} are closed; V_2,V_4,V_6 are opened.

84 The HTS_1 is heated by the heat source and ammonia vapour flows to the expander. The
85 high pressure ammonia drives the expander to produce electricity while the LTS_1 adsorbs
86 ammonia and rejects the adsorption heat to the environment such as a cooling tower. On
87 the other side of this system, the HTS_2 adsorbs the ammonia from LTS_2 where the
88 refrigeration can be obtained. Step 2 is working as a mirror stage of step 1, where the
89 HTS_2 is heated by the heat source and the LTS_1 generates refrigeration. The V_1,V_3,V_5 are
90 opened and V_2, V_4,V_6,V_{m1},V_{m2} are closed in step 2, which is illustrated in Fig. 1(b).

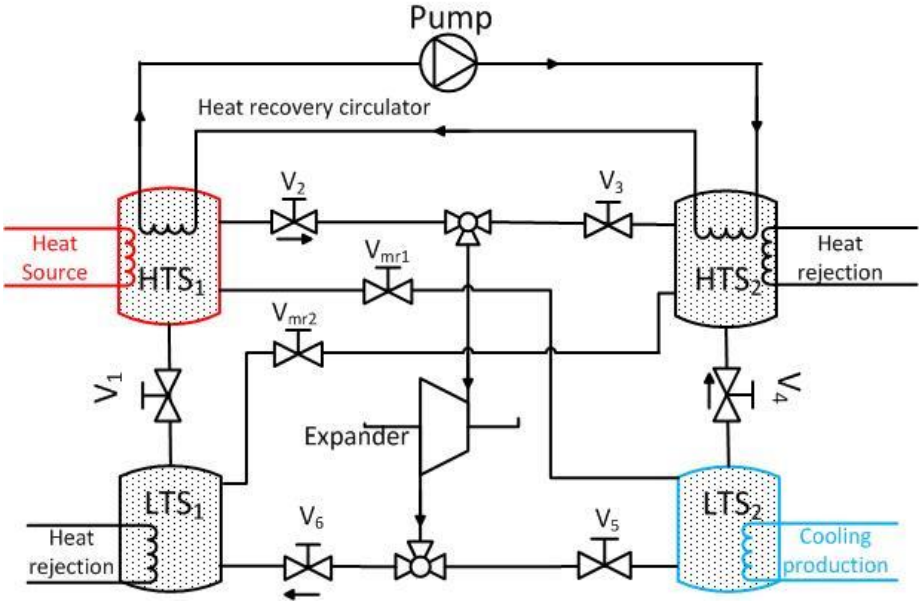

Step1 (a)

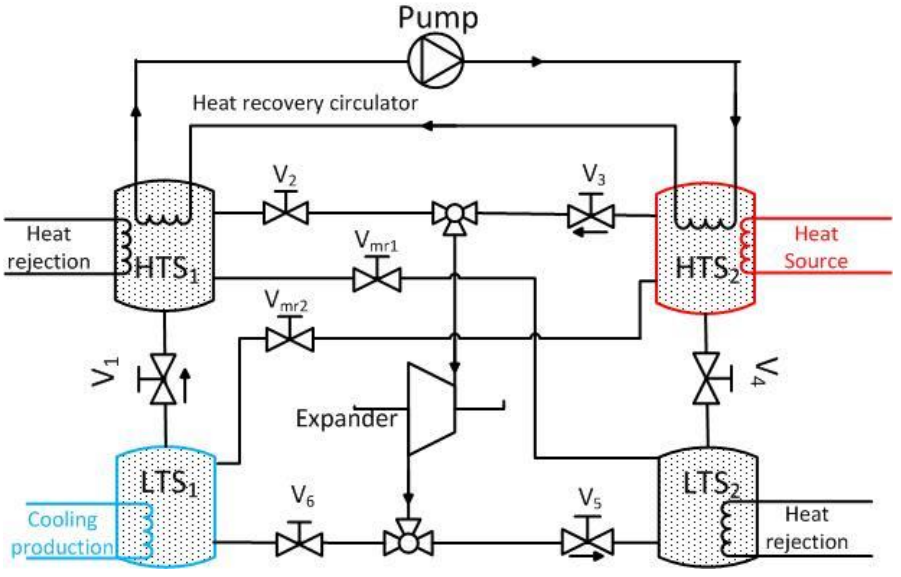

Step 2 (b)

Fig. 1. Schematic diagram of a resorption cogeneration applying heat recovery process (a) Step 1, HTS_1 & LTS_1 power generation, HTS_2 & LTS_2 refrigeration generation; (b) Step 2 HTS_1 & LTS_1 refrigeration generation, HTS_2 & LTS_2 power generation

91

92 Three HTS ($NiCl_2$, $FeCl_3$, $MnCl_2$) and four LTS ($BaCl_2$, $PbCl_3$, $CaCl_2$, $SrCl_2$) are chosen to

93 be analysed in the resorption cogeneration. Their reaction equations are list as follows,

$$NiCl_2 \cdot 2NH_3 + 4NH_3 \Leftrightarrow NiCl_2 \cdot 6NH_3 + 4\Delta H_{NiCl_2} \quad (1)$$

$$FeCl_3 \cdot 2NH_3 + 4NH_3 \Leftrightarrow FeCl_3 \cdot 6NH_3 + 4\Delta H_{FeCl_3} \quad (2)$$

$$MnCl_2 \cdot 2NH_3 + 4NH_3 \Leftrightarrow MnCl_2 \cdot 6NH_3 + 4\Delta H_{MnCl_2} \quad (3)$$

$$SrCl_2 \cdot NH_3 + 7NH_3 \Leftrightarrow SrCl_2 \cdot 8NH_3 + 7\Delta H_{SrCl_2} \quad (4)$$

$$CaCl_2 \cdot 4NH_3 + 4NH_3 \Leftrightarrow CaCl_2 \cdot 8NH_3 + 4\Delta H_{CaCl_2} \quad (5)$$

$$BaCl_2 + 8NH_3 \Leftrightarrow BaCl_2 \cdot 8NH_3 + 8\Delta H_{BaCl_2} \quad (6)$$

$$PbCl_2 \cdot 3.25NH_3 + 4.75NH_3 \Leftrightarrow PbCl_2 \cdot 8NH_3 + 4.75\Delta H_{PbCl_2} \quad (7)$$

The equilibrium reaction lines and thermodynamic features of the resorption cogeneration are shown in Fig.2. Line A-B is the heating process of the ammonia inside the HTS, where Point B and Point A are on the equilibrium reaction line of the HTS. The isentropic expansion process is represented by line B-C. The refrigeration generation is achieved from Line D-A and the refrigeration temperature of the system is T_D. In this paper, the environmental temperature is set at 20 ^oC.

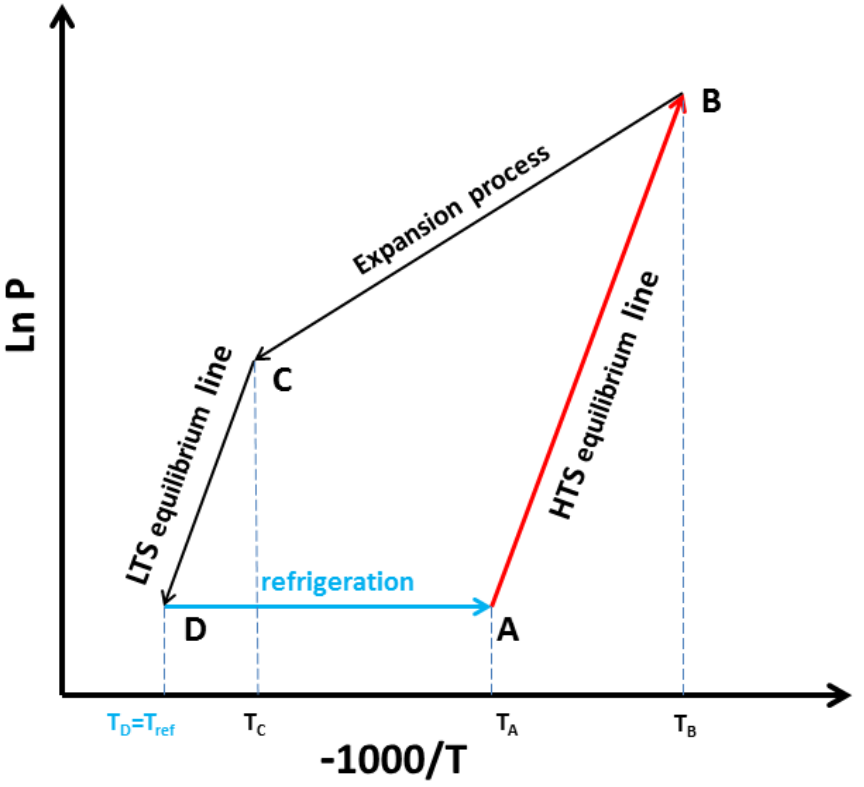

Fig.2. Clausius-Clapeyron diagram of the resorption cogeneration

2.2 Heat recovery process

To regenerate the sensible heat from HTS after the heating process, a separate circulator is added between the HTS_1 and the HTS_2. The heat recovery process applies between the Step 1 and the Step 2 during the switch time. Fig. 3 (a) illustrates the principle of the heat recovery process, when the system switches from Step 2 to Step 1. Line 3-6 is the heat

removed from one of the HTS to preheat the other HTS from Point 1 to Point 5. In ideal heat recovery process, the temperature of Point 5 is the same as the temperature of Point 6 (T_5=T_6=T_{hr}). The P-T diagrams of the heat recovery process between two HTS are shown in Fig. 3.

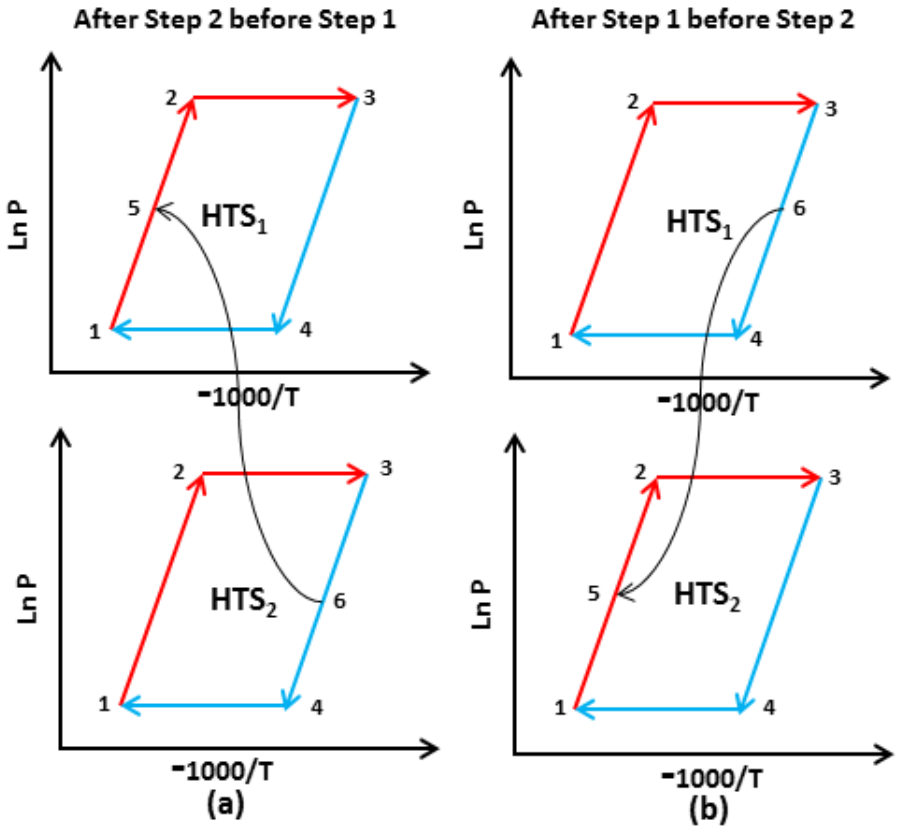

Fig.3. P-T diagram for the heat recovery process between HTS_1 and HTS_2 (a) after Step2 before Step1 (b) After Step 2 before Step 1

2.3 Mass recovery process

To further improve the refrigeration generation, mass recovery process is introduced here to equalise the pressures of the four adsorbent beds. In the end of step 1, the pressure of

the HTS_1 is higher than the saturated pressure under heat source temperature. Meanwhile the pressure of the LTS_2 is lower than the saturated pressure under refrigeration temperature. During the mass recovery process, all valves need to be switched off except V_{mr1}. The Vmr1 only needs to be switched on for 10 seconds to let ammonia evaporating from the HTS1 into the LTS2. The further obtained ammonia into the LTS2 can be represented as line E-E′ in Fig. 4. This equalisation process not only can speed up these two beds reaching their saturation state but also increase the total mass flows into the system. In the end of this equalisation process, the mass recovery valve Vmr1 needs to be switched off. The further achieved refrigeration is obtained from the LTS2 by switching on the V4, when the ammonia desorbs from the LTS2 and adsorbed by the HTS1. The dash dot lines present the mass recovery process as shown in Fig. 4.

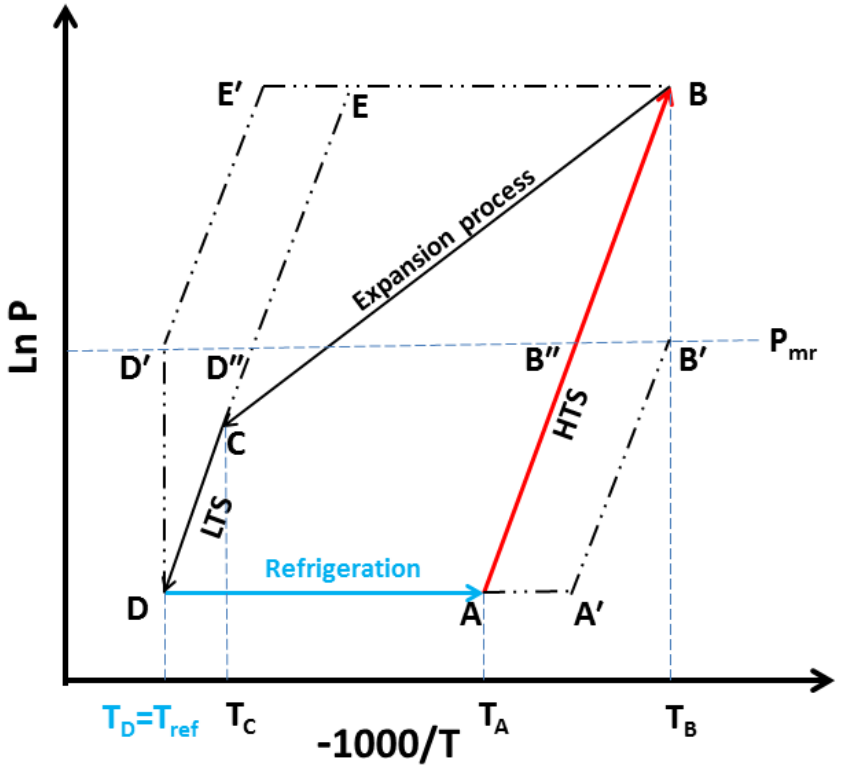

Fig. 4. P-T diagram of the mass recovery process between the HTS_1 and the LTS_2

Several assumptions are applied here for the analysis of the mass recovery process.

1. The processes B-B′ and D-D′ are recognised as isothermal processes. ($T_B=T_{B'}$, $T_D=T_{D'}$)
2. The further desorbed ammonia from the HTS_1 is fully adsorbed by the LTS_2. ($\Delta x_{D-D'}=\Delta x_{B-B'}$)
3. By using mass recovery process, the final pressure state of the HTS_1 is equivalent to that of the LTS_2. ($P_{B'}=P_{D'}=P_{mr}$)
4. Point B″ and Point D″ are on the equilibrium lines of HTS and LTS. The temperature difference between Point B′ and Point B″ is the same as that between Point D′ and Point D″. ($T_{B'}-T_{B''}=T_{D''}-T_{D'}$)
5. The extra adsorption heat, which is caused by the mass recovery process, needs to be rejected to the environment is shown as Line A-A′ in Fig. 4. The temperature increase of the HTS_2 equal to the temperature difference between Point B′ and Point B″. ($T_A-T_{A'}=T_{B'}-T_{B''}$)
6. The chemical reaction can be 100% completed without considering the reaction time.

3. Analysis

The total heat input includes the reaction heat and the sensible heat of the adsorbent, which is described by equation (8). m_{am} is the total mass of the adsorption/desorption ammonia between the HTS and the LTS.

$$\begin{aligned} Q_h &= m_{am}\times\Delta x\times\Delta h_{HTS}+m_{am}\times\Delta u_{HTS} \\ &= m_{am}\times\Delta x\times\Delta h_{HTS}+m_{HTS}\times c_{pHTS}\times(T_h-T_0)+m_{am}\times c_{pam}\times(T_h-T_0) \end{aligned} \tag{8}$$

The refrigeration generation includes the sensible heat for LTS to cool down at refrigeration temperature and the chemical reaction heat producing cooling.

$$Q_{ref} = m_{am} \times \Delta x \times \Delta h_{LTS} + m_{am} \times \Delta u_{LTS}$$
$$= m_{am} \times \Delta x \times \Delta h_{LTS} - m_{LTS} \times c_{pLTS} \times (T_0 - T_{ref}) - m_{am} \times c_{pam} \times (T_0 - T_{ref}) \quad (9)$$

148 The heat recovered by the heat recovery process can be calculated as

$$Q_{hr} = (Q_{hr\_HTS1} + Q_{hr\_HTS2}) \div 2$$
$$= [m_{HTS} \times c_{pHTS} \times (T_B - T_{hr}) + m_{am} \times c_{pam} \times (T_B - T_{hr}) * (1 - \Delta x) \quad (10)$$
$$+ m_{HTS} \times c_{pLTS} \times (T_{hr} - T_0) + m_{am} \times c_{pam} \times (T_{hr} - T_0) * \Delta x] \div 2$$

149 The isentropic expansion process inside the expander is calculated by the enthalpy
150 difference between Point B and Point C.

$$W = m_{am} \times \Delta x \times (h_B - h_C) \quad (11)$$

151 The extra cooling production caused by the mass recovery process is described as

$$Q_{ref\_mr} = m_{am} \times (1 - \Delta x) \times \Delta h_{LTS} + m_{am} \times \Delta u'_{LTS}$$
$$= m_{am} \times (1 - \Delta x) \times \Delta h_{LTS} - m_{LTS} \times c_{pLTS} \times (T_{D'} - T_{ref}) - m_{am} \times c_{pam} \times (T_{D'} - T_{ref}) \quad (12)$$

152 The coefficient of performance (COP) of the resorption system without mass and heat
153 recovery is

$$COP = Q_{ref} \div Q_h \quad (13)$$

154 With mass recovery process only

$$COP_{mr} = (Q_{ref} + Q_{ref\_mr}) \div Q_h \quad (14)$$

155 With heat recovery process only

$$COP_{hr} = Q_{ref} \div (Q_h - Q_{hr}) \quad (15)$$

156 With mass and heat recovery

$$COP_{mr\&hr} = (Q_{ref} + Q_{ref\_mr}) \div (Q_h - Q_{hr}) \quad (16)$$

157 The power generation performance with and without heat recovery process are calculated
158 by

$$\eta_{I\_ele} = W \div Q_h \tag{17}$$

$$\eta_{I\_ele\_hr} = W \div (Q_h - Q_{hr}) \tag{18}$$

159 The second law analysis is applied in this study to evaluate the utilization of useful work
160 from this resorption cogeneration. The exergy from the heat source of the resorption
161 cogeneration applying mass and heat recovery is defined as

$$\begin{aligned} E_{h\_mr\&hr} &= E_h - E_{h\_hr} \\ &= m_{am} \times [(h_B - h_0) - T_0 \times (s_B - s_0)] - m_{am} \times [(h_{hr} - h_0) - T_0 \times (s_{hr} - s_0)] \end{aligned} \tag{19}$$

162 Due to the chemical reaction process for refrigeration generation, the refrigeration exergy
163 is calculated by

$$E_{ref\_mr\&hr} = E_{ref} + E_{ref\_mr} = (Q_{ref} + Q_{ref\_mr}) \times (T_0 / T_{ref} - 1) \tag{20}$$

164 The second law efficiency of the electricity generation part from this system is

$$\eta_{II\_ele} = W \div E_{h\_mr\&hr} \tag{21}$$

165 The second law efficiency for refrigeration process is

$$\eta_{II\_ref} = E_{ref\_mr\&hr} \div E_{h\_mr\&hr} \tag{22}$$

166 The overall system evaluation by the second law analysis is

$$\eta_{II\_total} = \eta_{II\_ele} + \eta_{II\_ref} \tag{23}$$

167

168 Table 1

169 Thermodynamic parameters for the chosen salts and ammonia

Molecular formula	ΔH (J/mol)	ΔS [J/(mol·K)]	C_p[J/(mol ·K)]	M (g/mol)	Reaction salt with per mol ammonia (g)
NH_3	22839	191.39	80.27(liquid)	17.03	

$PbCl_2$(8-3.25)	34317	223.76	70.05	278.1	57.34
$BaCl_2$(8-0)	37665	227.25	75.1	208.23	26.03
$CaCl_2$(8-4)	41013	230.3	72.52	110.98	27.74
$SrCl_2$(8-1)	41431	228.8	75.53	158.53	22.65
$MnCl_2$(6-2)	47416	228.07	72.86	125.84	31.46
$FeCl_3$(6-2)	51266	227.99	76.57	162.2	40.55
$NiCl_2$(6-2)	59217	227.75	71.6	129.6	32.40

4. Results and Discussions

4.1 Selection of the resorption working pair

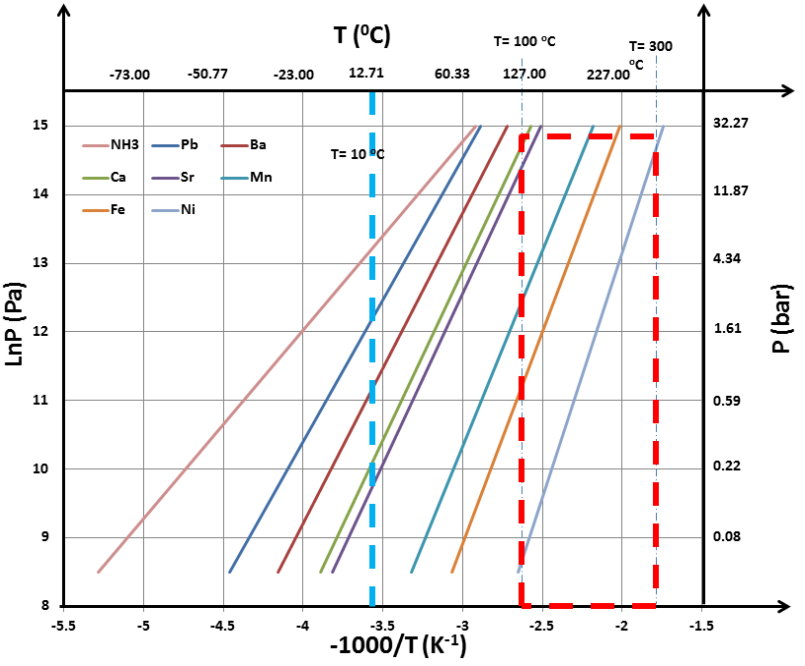

Fig. 5. Equilibrium lines of selected salts and ammonia in P-T diagram

For chemisorption adsorption, the final state inside each salt will reach the point on the equilibrium lines, which is shown in Fig. 5. In this study, the temperature of the heat

source is chosen from 100 ^{0}C to 300 ^{0}C and the refrigeration temperatures are set at 10 ^{o}C. The promising LTS and HTS for the resorption cogeneration are $PbCl_2$, $BaCl_2$, $CaCl_2$, $SrCl_2$ as LTS and $MnCl_2$, $FeCl_3$, $NiCl_2$ as HTS. To simplify the system design and reduce the construction cost, the highest system pressure is set at 40 bar. The pressures of the three HTS candidates under 40 bar are listed in Table 2. A minimum start pressure (the pressure difference between the HTS and the LTS) is set at 100 kPa to ensure the electrical generation from the scroll expander. In another word, the pressure difference between the HTS (in desorption process under heat source temperature) and the LTS during (in adsorption process cooled down to the environmental temperature) needs to be higher than 100kPa. The pressures of the LTS under the refrigeration temperature (10 ^{o}C) and environmental temperature (20 ^{o}C) are listed in Table 3.

Table 2

Equilibrium pressure of the HTS under different heating temperatures

Heat source temperature (^{o}C)	P_{MnCl2} (kPa)	P_{FeCl3} (kPa)	P_{NiCl2} (kPa)
100	188.70	53.97	
110	281.35	83.12	
120	411.03	125.23	
130	589.30	184.88	
140	830.28	267.83	
150	1150.99	381.26	38.58
160	1571.68	533.95	56.92
170	2116.17	736.51	82.53

180	2812.12	1001.58	117.72
190	3691.33	1344.09	165.35
200		1781.43	228.94
210		2333.69	312.74
220		3023.85	421.84
230		3877.96	562.28
240			741.12
250			966.57
260			1248.12
270			1596.56
280			2024.18
290			2544.79
300			3173.84

Table 3

Equilibrium pressure of the LTS at environmental temperature and refrigeration temperature

T (^{o}C)	P_{PbCl2} (kPa)	P_{BaCl2} (kPa)	P_{CaCl2} (kPa)	P_{SrCl2} (kPa)
20	374.14	143.96	52.54	36.94
10	227.38	83.34	28.97	20.25

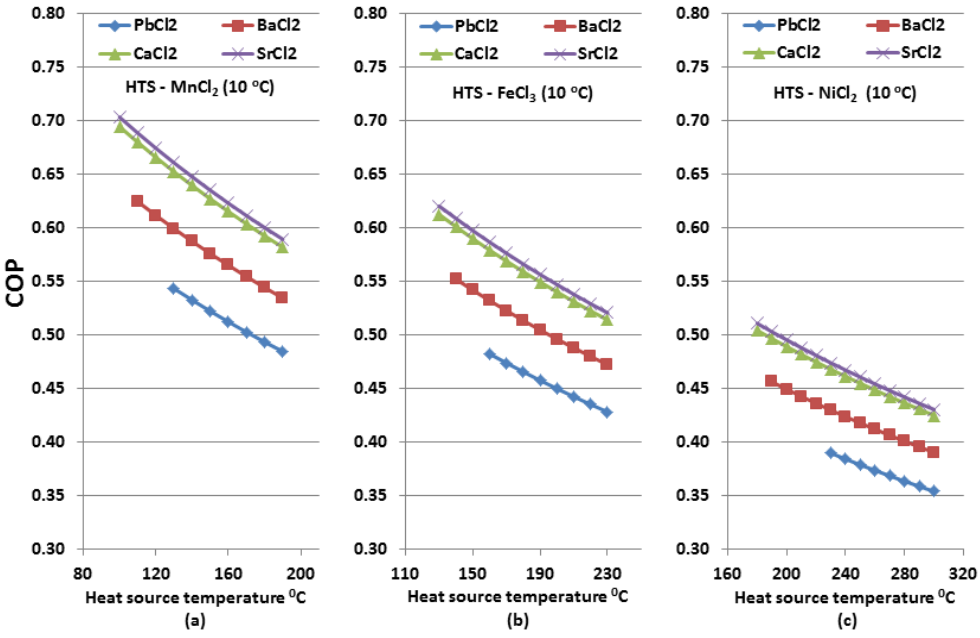

Fig. 6. Relationship between the COP and heat source temperature of the resorption cogeneration at 10 °C refrigeration temperature (a) HTS - $MnCl_2$; (b) HTS - $FeCl_3$; (c) HTS - $NiCl_2$

198

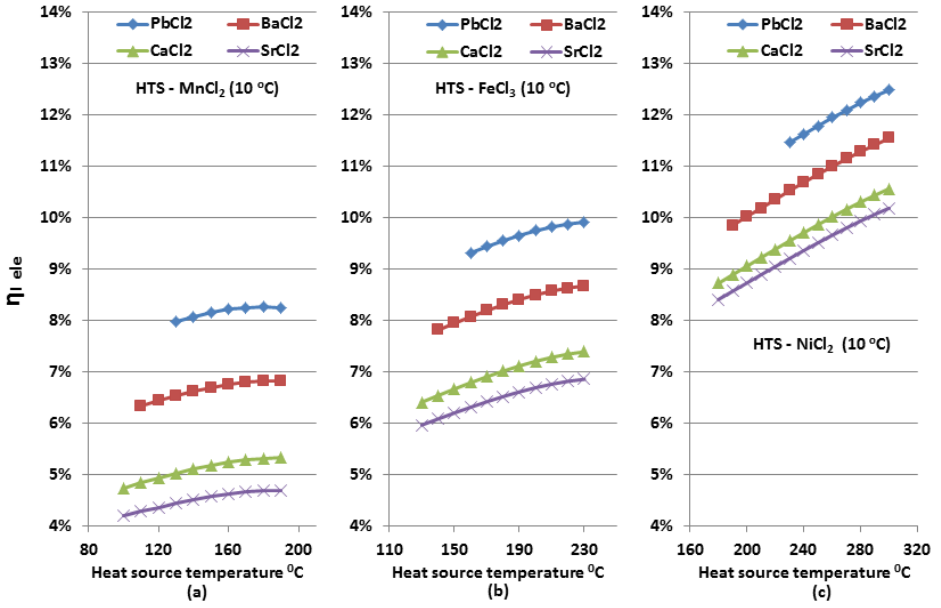

Fig. 7. Relationship between the energy efficiency of the electricity production and heat source temperature (a) HTS - $MnCl_2$; (b) HTS – $FeCl_3$; (c) HTS – $NiCl_2$

In this study, the sorption quantity (Δx) is assumed at 80%. The refrigeration performance at 10 ^{o}C of this resorption cogeneration is calculated by equation (13) and the results are shown in Fig. 6. Among the twelve resorption pairs, the COP of this system declines with the increase of the heat source temperature. The highest heating temperature of the chosen high temperature salts is 190 ^{o}C for $MnCl_2$, 240 ^{o}C for $FeCl_3$ and 300 ^{o}C for $NiCl_2$. The pressure of $PbCl_2$ at 20 ^{o}C is as high as 374.14 kPa, which is the highest among the four LTS candidate. Therefore $PbCl_2$ requires relatively high supply pressure from the HTS, which will limit the system flexibility. The highest COP is achieved at 0.70 by the $SrCl_2$-$MnCl_2$ working pair with the heating temperature at 100 ^{o}C.

The energy efficiency of the electricity generation with the increase of the heat source temperature is shown in Fig. 7. The ammonia enthalpy at the inlet and the outlet of the expander determines the power generation performance, which is calculated by equation (11). Among the four LTS candidates, the $PbCl_2$ shows a competitive performance during the power generation part. The electrical energy efficiency of the resorption working pair $PbCl_2$-$MnCl_2$, $BaCl_2$-$MnCl_2$, $CaCl_2$-$MnCl_2$ and $SrCl_2$-$MnCl_2$ is around 8.2%, 6.5%, 5.0% and 4.5%, respectively. Under the same working conditions, the electrical energy efficiency of the resorption cogeneration using HTS-$FeCl_3$ is higher than that using HTS-$MnCl_2$. The $PbCl_2$-$NiCl_2$ achieves the highest electrical energy efficiency at 12.49% under the heat source temperature at 300 ^{o}C. However, the weight of reaction adsorbents also needs to be considered to simplify the system design and reduce the construction cost. Based on the adsorption reaction equations (1) - (7), the reaction weight of salts with per mol ammonia is listed in Table 1.

In summary, this resorption cogeneration can be used under the heat source temperature from 100 ^{o}C to 300 ^{o}C using different HTS ($MnCl_2$, $FeCl_3$ or $NiCl_2$). The $FeCl_3$ has the highest reaction weight with 1 mol ammonia among the three HTS, which is not preferred in the system. Therefore the $MnCl_2$ and $NiCl_2$ are chosen as the optimal HTS for further

225 analysis. For the selection of LTS, the performance of power and refrigeration generation
226 of the cogeneration using $SrCl_2$ and $CaCl_2$ are quite close, which are shown in Fig. 6 and
227 Fig. 7. The $SrCl_2$ who has a lower reaction weight with per mol ammonia can be selected
228 as a representative for $CaCl_2$. The $PbCl_2$, who needs higher supply pressure and higher
229 reaction weight with one mol ammonia compared with the other LTS candidates, is not
230 suggested to be used as the LTS in this system.
231 To investigate the effect of mass and heat recovery processes for this resorption
232 cogeneration, the COP and electrical energy efficiency of this resorption system using four
233 optimised working pairs are conducted and discussed in the next section.
234
235 4.2 Heat and mass recovery

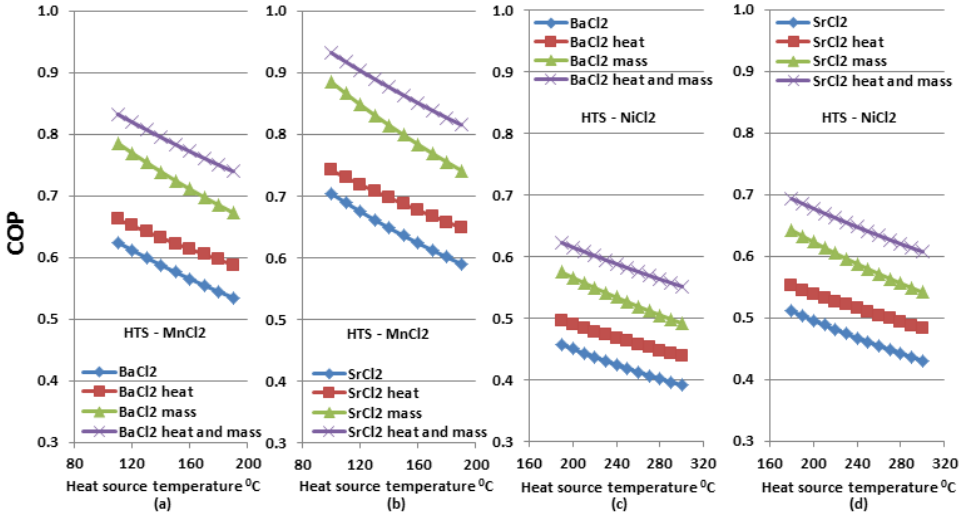

Fig. 8. COP of the resorption with working pair
(a) $BaCl_2$-$MnCl_2$; (b) $SrCl_2$-$MnCl_2$; (c) $BaCl_2$-$NiCl_2$; (d) $SrCl_2$-$NiCl_2$
236

237 To further improve the system performance, heat recovery and mass recovery process are
238 introduced here. The Fig. 8 shows the COP improvement of the system applying heat
239 recovery, mass recovery and heat/mass recovery. Results suggest that all of these three
240 methods can effectively improve the refrigeration performance. The COP entrancement

with mass recovery is higher than that with heat recovery, which means the mass recovery has a more important role than the heat recovery for refrigeration generation in this system. For the working pairs $BaCl_2$ – $MnCl_2$ and $SrCl_2$ – $MnCl_2$, their COP are both improved by 35% with the help of heat/mass recovery. Under the heat source temperature from 110 ^oC to 190 ^oC, the COP of the system with $SrCl_2$ – $MnCl_2$ as working pair is around 0.85 which is higher than that of the system with $BaCl_2$-$MnCl_2$ working pair. The COP enhancement of the other two resorption working pairs BaCl2-NiCl2 and SrCl2-NiCl2 also show effectively improved by 38% after applying heat/mass recovery.

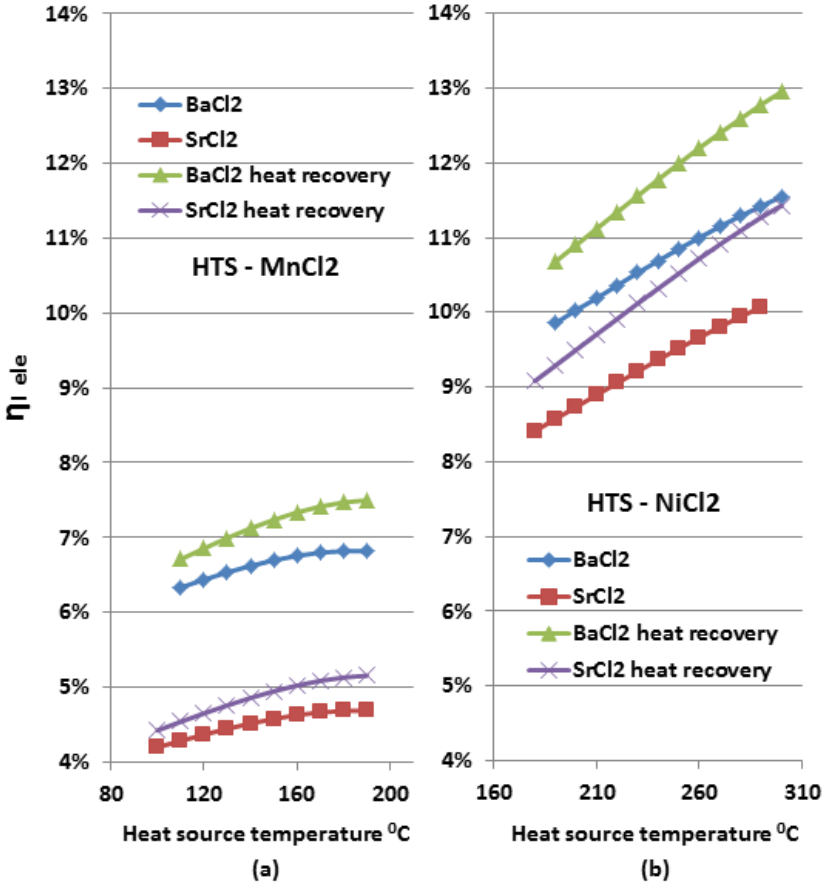

Fig. 9. Electrical energy efficiency of the resorption working pair (a) $BaCl_2$-$MnCl_2$ and $SrCl_2$-$MnCl_2$; (b) $BaCl_2$-$NiCl_2$ and $SrCl_2$-$NiCl_2$

The heat recovery also improves the system performance for electricity generation, which is shown in Fig.9. It can be seen that heat recovery can effectively increase the electrical energy efficiency of this resorption cogeneration. With increasing heat source temperature, the contribution rate from the recovered heat is higher than that from the electricity generation. Therefore the slope of the electrical energy efficiency line using heat recovery is greater than that of original system. Although heat recovery cannot increase the power produced from this system, the electrical energy efficiency of this system using $MnCl_2$ and $NiCl_2$ as HTS is improved by 8% and 12%, respectively.

To further evaluate the performance of the resorption cogeneration, second law analysis is applied in the following section.

4.3 Second law analysis

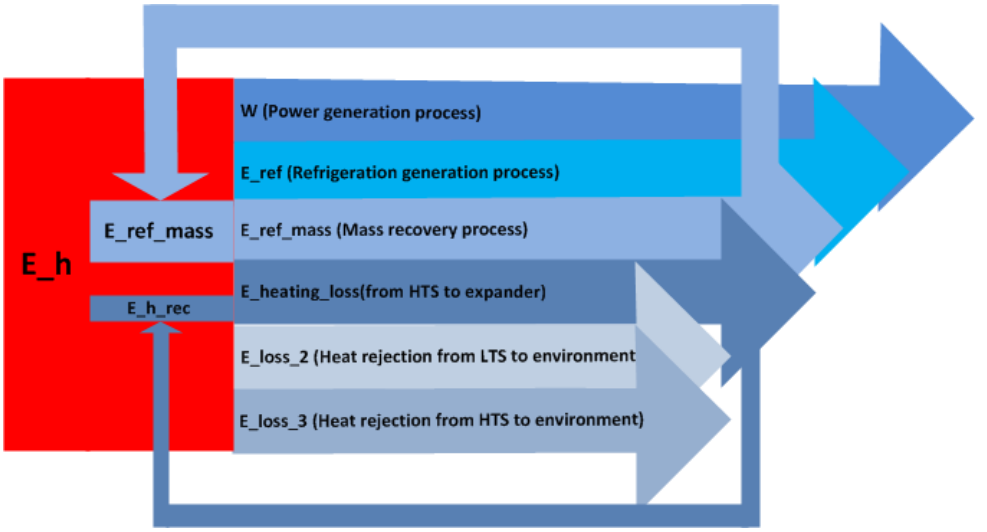

Fig. 10 Exergy flow chart of the resorption cogeneration applying mass and heat recovery

Table. 4

Exergy destruction comparison between two cases

	Case 1 BaCl2-MnCl2 at 150 oC		Case 2 BaCl2-NiCl2 at 250 oC	
	Exergy (J/kg)	Ratio of Exergy to Total Exergy (%)	Exergy (J/kg)	Ratio of Exergy to Total Exergy (%)
	Total Exergy			
Heat input (E_h)	15593	100%	30763	100%
	Exergy Destruction			
Heating loss (E_{hl})	3439	22.06%	8133	26.44%
Heat rejection ($E_{hl\_LTS} + E_{hl\_HTS}$)	7716	49.49%	14004.3	45.50%
	Exergy Output			
Power (W)	3397	21.79%	7587	24.66%
Refrigeration (E_{ref})	1033	6.62%	1033	3.36%
	Exergy Recovery			
Heat recovery (E_{hr})	688.6	4.42%	1181	6.12%
Mass recovery (E_{ref_mr})	266.1	1.17%	266.1	0.86%

To have a better understanding of the exergy utilisation of this novel resorption cogeneration, the exergy flow chart is shown in Fig. 10. The total exergy input is coming from the heating process of the HTS. The exergy destructions include the exery loss during the heating process from HTS to the inlet of the expander, adsorption heat rejection from the LTS to the environment and adsorption heat rejection from the HTS to the environment. The heat recovered from HTS1 to HTS2 and the refrigeration recovered from the mass recovery process can be seen from Fig. 10.

Two cases are studied to investigate the key processes of this system. Results are listed in Table 4. The majority of exergy destructions are coming from the adsorption processes of the LTS and HTS, where the adsorption heat is released to the environment. There is 49.49% of the exergy released of BaCl2-MnCl2 working pair and 45.50% of the exergy released of BaCl2-NiCl2. The heat loss from the heating process of the HTS is around 22% and 26% in case 1 and case 2, respectively. Results also show the heat recovery can recover around 20% of the heat loss during the heating process to regenerate the heat. The

effect of the mass recovery for exergy utilisation is 1.17% and 0.86 in case 1 and case 2, respectively.

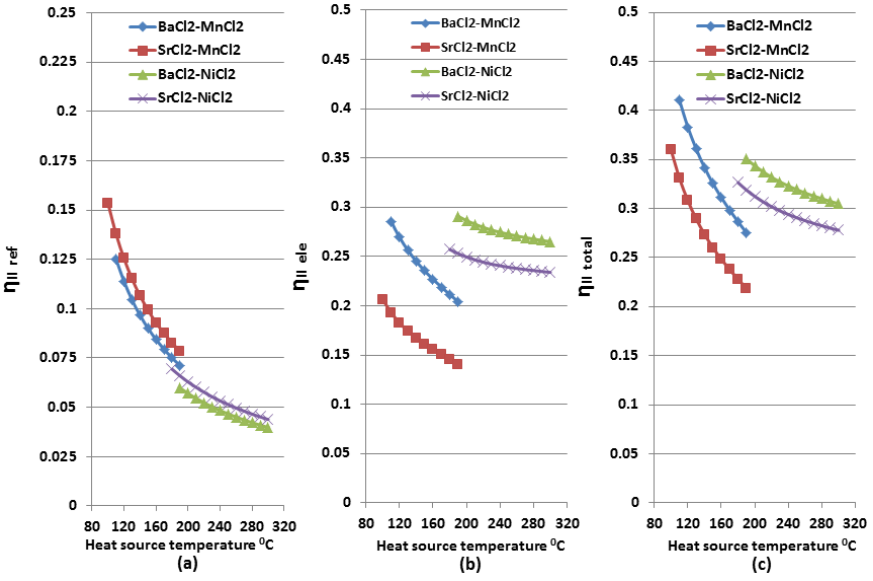

Fig. 11. Second law efficiency of the resorption cogeneration using HTS-$MnCl_2$, $NiCl_2$ and LTS-$BaCl_2$,$SrCl_2$
(a) refrigeration generation; (b) electricity generation;
(c) refrigeration and electricity generation

The second law efficiency of refrigeration generation, electricity generation and the combined generation is plotted in Fig. 11. In this study, the refrigeration generation is only determined by the conversion rate of ammonia without considering the cycle time. Therefore the second law efficiency for refrigeration generation decreases with the increase of heat source temperature. When the resorption working pair is $BaCl_2$- $MnCl_2$, the second law efficiency for electricity generation can reach as high as 0.28. The second law efficiency for electricity generation decreases with the increase of heat source temperature, which can be seen from the Fig. 11(b). Compared with the refrigeration generation, the electricity generation consumes more useful work in the system, which can be observed from the tendency of the second law efficiency in Fig. 11(b) and Fig. 11(c).

The highest second law efficiency obtained by the cogeneration is as high as 0.41 by the resorption working pair ($BaCl_2$-$MnCl_2$) at 110 ^oC heat source temperature. Although the $SrCl_2$-$MnCl_2$ shows better performance than the $BaCl_2$-$MnCl_2$ in refrigeration part, the second law efficiency for power generation achieved by the working pair $BaCl_2$-$MnCl_2$ is around 46% higher than that of the $SrCl_2$-$MnCl_2$. The overall exergy efficiency of this optimal resorption cogeneration is around 0.30 under the heat source temperature from 100 ^oC to 300 ^oC.

5. Conclusion

Analysis of this resorption cogeneration shows attractive performance for refrigeration and electricity generation under the heat source temperature ranging from 100 ^oC to 300 ^oC. First law analysis is applied to choose the optimal resorption working pairs from twelve candidates. Considering about the start pressure for the expansion machine, three HTS candidates are analysed to fit different heat source temperature application. Under the heat source temperature at 110 ^oC, the system without using mass and heat recovery can achieve its highest COP at 0.70 using $SrCl_2$-$MnCl_2$ as working pair. The highest electrical energy efficiency is achieved at 12.49% by the working pair PbCl2-$NiCl_2$ under 300 ^oC heat source temperature.

Four resorption working pairs are selected to be further calculated and compared with applying mass and heat recovery after considering the results from the first law analysis and reaction weight of the salts with per mol ammonia. Results show the mass recovery has a more critical effect on the refrigeration generation than the heat recovery. The exergy destruction analysis indicates that the majority of exergy losses are coming from the adsorption processes of the HTS and LTS, when the adsorption heat is rejected to the environment. The combined heat and mass recovery improves the COP by 35% for the HTS-MnCl2 and by 38% for the HTS-NiCl2. Furthermore, the percent increase of

electrical energy efficiency is from 8% to 12%, while the heat recovery is applied. The highest overall system law efficiency is achieved at 0.41 by the resorption working pair ($BaCl_2$-$MnCl_2$) with 110 ºC heat source temperature. This cogeneration shows a potential application to recovery low grade heat such as solar energy and industry waste heat into refrigeration and electricity. This system can be applied for either small-scale or large-scale application with the advantages of simple construction, dual energy generation, high COP, wide flexibility for different heat source temperature, etc.

Acknowledgement

The financial support of EPSRC through grant LH Cogen (EP/I027904/1) and Global SECURE (EP/K004689/1) is gratefully acknowledged. The first author would also like to thank for the partial financial support from the Henry Lester trust.

Reference

[1] Kalina AI. Combined cycle and waste-heat recovery power systems based on a novel thermodynamic energy cycle utilising low temperature heat for power generation. American Society of Mechanical Engineers Paper. 1983;83-JPGC-GT-3.

[2] Bombarda P, Invernizzi CM, Pietra C. Heat recovery from Diesel engines: A thermodynamic comparison between Kalina and ORC cycles. Applied Thermal Engineering. 2010;30:212-9.

[3] Campos Rodríguez CE, Escobar Palacio JC, Venturini OJ, Silva Lora EE, Cobas VM, Marques dos Santos D, et al. Exergetic and economic comparison of ORC and Kalina cycle for low temperature enhanced geothermal system in Brazil. Applied Thermal Engineering. 2013;52:109-19.

[4] Öhman H, Lundqvist P. Comparison and analysis of performance using Low Temperature Power Cycles. Applied Thermal Engineering. 2013;52:160-9.

[5] Walraven D, Laenen B, D'haeseleer W. Comparison of thermodynamic cycles for power production from low-temperature geothermal heat sources. Energy Conversion and Management. 2013;66:220-33.

[6] Zhang X, He M, Zhang Y. A review of research on the Kalina cycle. Renewable and Sustainable Energy Reviews. 2012;16:5309-18.

[7] Tamm G, Goswami DY, Lu S, Hasan AA. Theoretical and experimental investigation of an ammonia–water power and refrigeration thermodynamic cycle. Solar Energy. 2004;76:217-28.

[8] Sadrameli SM, Goswami DY. Optimum operating conditions for a combined power and cooling thermodynamic cycle. Applied Energy. 2007;84:254-65.

[9] Hasan AA, Goswami DY, Vijayaraghavan S. First and second law analysis of a new power and refrigeration thermodynamic cycle using a solar heat source. Solar Energy. 2002;73:385-93.

[10] Spinner B. Ammonia-based thermochemical transformers. Heat Recovery Systems and CHP. 1993;13:301-7.

[11] Wang LW, Bao HS, Wang RZ. A comparison of the performances of adsorption and resorption refrigeration systems powered by the low grade heat. Renewable Energy. 2009;34:2373-9.

[12] Li TX, Wang RZ, Kiplagat JK, Chen H. Experimental study and comparison of thermochemical resorption refrigeration cycle and adsorption refrigeration cycle. Chemical Engineering Science. 2010;65:4222-30.

[13] H.S. Bao, Wang RZ. A review of reactant salts for resorption refrigeration systems. International Journal of Air-Conditioning and Refirgeration. April 2010;18:165-80.

[14] Bao HS, Oliveira RG, Wang RZ, Wang LW, Ma ZW. Working pairs for resorption refrigerator. Applied Thermal Engineering2011. p. 3015-21.

[15] Wang L, Ziegler F, Roskilly AP, Wang R, Wang Y. A resorption cycle for the cogeneration of electricity and refrigeration. Applied Energy. 2013;106:56-64.

[16] Oliveira RG, Silveira Jr V, Wang RZ. Experimental study of mass recovery adsorption cycles for ice making at low generation temperature. Applied Thermal Engineering. 2006;26:303-11.

[17] Wang LW, Wang RZ, Lu ZS, Chen CJ, Wu JY. Comparison of the adsorption performance of compound adsorbent in a refrigeration cycle with and without mass recovery. Chemical Engineering Science. 2006;61:3761-70.

[18] Akahira A, Alam KCA, Hamamoto Y, Akisawa A, Kashiwagi T. Experimental investigation of mass recovery adsorption refrigeration cycle. International Journal of Refrigeration. 2005;28:565-72.

[19] Akahira A, Alam KCA, Hamamoto Y, Akisawa A, Kashiwagi T. Mass recovery adsorption refrigeration cycle—improving cooling capacity. International Journal of Refrigeration. 2004;27:225-34.

[20] Wang RZ. Performance improvement of adsorption cooling by heat and mass recovery operation. International Journal of Refrigeration. 2001;24:602-11.